Rev.Adv.Mater.Sci. 25 (2010) 1-10

TOWARDS ENHANCEMENT OF PROPERTIES OF UFG METALS AND ALLOYS BY GRAIN BOUNDARY ENGINEERING USING SPD PROCESSING

R.Z. Valiev, I.V. Alexandrov, N.A. Enikeev, M.Yu. Murashkin and I.P. Semenova

Institute of Physics of Advanced Materials, Ufa State Aviation Technical University, 12 K. Marx str., Ufa 450000, Russia

Received: December 15, 2009

Abstract. Nanostructuring of metals and alloys by severe plastic deformation techniques is an effective way of enhancing their mechanical and functional properties. The features of the nanostructured materials produced by severe plastic deformation are stipulated by forming of ultrafine-sized grains as well as by the state of grain boundaries. The concept of grain boundary engineering of ultrafine-grained metals and alloys is developed for enhancement of their properties by tailoring grain boundaries of different types (low-angle and high-angle ones, special and random, equilibrium and nonequilibrium) and formation of grain boundary segregations and precipitations by severe plastic deformation processing. In this article, using this approach and varying regimes and routes of severe plastic deformation processing, we show for several light alloys (Al and Ti) the ability to produce ultrafine-grained materials with different grain boundaries, and this can have a drastic effect on the mechanical behavior of the processed materials. This article demonstrates also several new examples of attaining superior strength and ductility as well as enhanced superplasticity at low temperatures and high strain rates in various ultrafine-grained metals and alloys.

1. INTRODUCTION

Ultrafine-grained (UFG) materials with a grain size in the submicrometer (100–1000 nm) or nanometer (less than 100 nm) range possess much higher area of grain boundaries than usual coarse-grained counterparts; that is why the properties of UFG materials depend considerably on the structure and behavior of internal interfaces – grain boundaries (GBs). Therefore, the UFG materials are commonly defined as interface-controlled materials [1]. At the same time in the UFG materials produced by severe plastic deformation (SPD) techniques the grain boundaries character might vary significantly depending on the regimes and routes of processing. The grain boundaries may be high- and low-angle, special and random, equilibrium and non-equilibrium ones as well as contain GB segregations or precipitations [2–7]. These features open a possibility to control and enhance the properties of UFG materials by variation of the GB structure using SPD processing. This approach can be considered as GB engineering of UFG metals and alloys [5,6].

Corresponding author: R.Z. Valiev, e-mail: rzvaliev@mail.rb.ru

The concept of GB engineering or GB design was introduced by T. Watanabe in [8] where it had been proposed that the properties of polycrystalline materials may be effectively changed by deliberate and careful tailoring of grain boundary character distribution. This approach has been used successfully for several studies including, for example, improving the susceptibility to intergranular stress corrosion cracking [9]. However, generally there are certain difficulties in achieving different boundary distributions in conventional coarse-grained materials. In this connection, UFG materials in which GB structure features are associated with SPD processing regimes provide extended possibilities for GB engineering.

Presently studies of grain boundaries in UFG materials is among high research topics, where special attention is given to modeling and experimental investigation of atomic structure of GB, defects formation at boundaries and their influence on the materials properties [2-7]. These works include the application of various processing techniques in order to produce nanostructured materials.

During last years in our laboratory a number of investigations has been performed dealing with nanostructuring of metals and alloys [2,10] by using two most popular SPD techniques – high-pressure torsion (HPT) and equal-channel angular pressing (ECAP), and with the focus on GB evolution. This paper reports several new examples of GB engineering for attaining enhanced strength and ductility, fatigue and superplasticity in the light UFG materials (Al and Ti).

2. EXPERIMENTAL PROCEDURE

The materials for this study were commercially pure titanium Grade 2 and Grade 4, Ti-6%Al-4%V ELI alloy and Al alloy 1570 (Al-5.7%Mg-0.32%Sc-0.4%Mn). UFG structure in these materials was formed by ECAP and HPT processing [11-13]. Microstructure of the processed materials was studied by TEM, X-ray diffraction, and SEM equipped with electron back-scatter diffraction (EBSD) facilities. The tensile tests at room temperature were carried out on flat small samples with a gage of $1\times0.25\times3$ mm and a strain rate of 3×10^{-4} s^{-1} using a specially designed tensile machine [14,15] and dynamometer "Instron" on standard cylindrical samples with a gage 3 mm in diameter and 15 mm in length. The samples for fatigue tests were cut along the rods. The working surface of smooth samples was ground and mechanically polished providing the roughness R_a = 0.63 μm. The tests were implemented under conditions of bending with rotation of f=50 Hz frequency according to ASTM E 466-96. The cycle asymmetry factor was $R(\sigma_{min}/\sigma_{max})$ = -1, the testing base was $NF = 10^7$ cycles.

3. RESULTS

3.1. The UFG commercially pure Ti

The evidence available to date shows that both ECAP and HPT processing provide an effective procedure for achieving different misorientation distributions. Indeed, there is a high fraction of low-angle boundaries after low applied strain (γ<4-5) and their fraction diminishes at the expense of high-angle ones with strain increasing [2,4,10]. For example, the HPT-processed Ti with γ>10 demonstrates homogeneous UFG structure formed predominantly by high angle grain boundaries with the average grain size of about 120 nm [15]. Such UFG structure is stable at heating up to 300 °C. Mechanical tensile tests demonstrated that strength and especially ductility of UFG Ti produced by HPT varies considerably with different applied strain [16], which clearly illustrates that the increase of the fraction of high-angle GBs contributes to the enhancement of mechanical properties of UFG CP Ti.

A new interesting example of GB engineering is investigation of mechanical behavior of UFG Ti produced by combined SPD processing in the shape of long-length rods. This novel technology of fabrication of rods up to 8 mm in diameter and up to 3 m in length from UFG Ti was developed in our laboratory and comprises ECAP with consequent thermomechanical treatment (TMT) [11]. Such combined SPD processing results in the formation of UFG structure in the rods that consists of equiaxed grains with size less that 150 nm (Fig. 1) though there are elongated grains in longitudinal direction with substructure inside the grains. Misorientation measurements by EBSD demonstrated that the fraction of high-angle GBs in the given state constitutes less than 40%. At the same time by variation of straining regimes and performing TMT at 450 °C we found a considerable reduction in substructure and increase in the fraction of high-angle GBs constituted up to 80% with maintenance of the average grain size (Fig. 2).

Fig. 3 shows the stress-strain curves of UFG Ti after ECAP and consequent TMT at different temperatures. It can be seen that straining at 450 °C with increase in the fraction of GBs with high-angle misorientations leads to considerable enhancement of stress flow and elongation to failure as well. It is

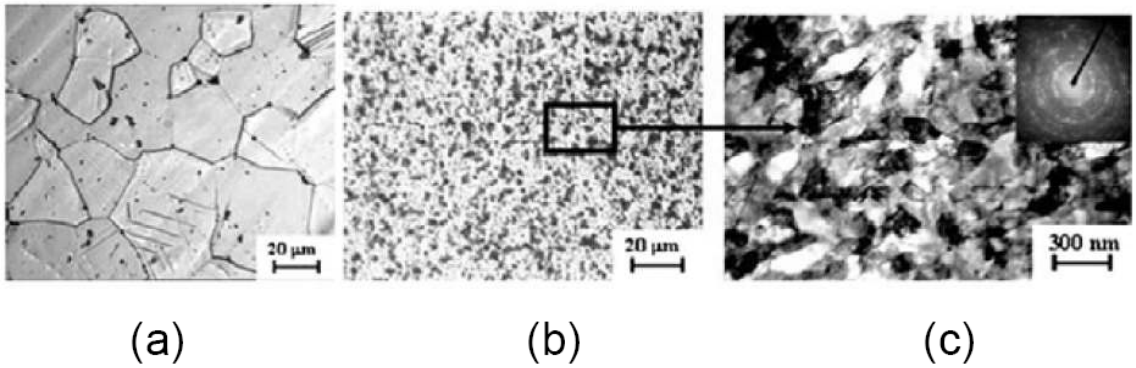

Fig. 1. Optical and transmission electron microscopy illustrating microstructure of CP Ti Grade 4: (a) conventional; (b, c) ECAP + TMT.

also very important that enhancement of strength and ductility can result in considerable enhancement of endurance limit. For example, we found the enhancement of endurance limit on the basis of 10^7 cycles from 610 to 640 MPa in UFG Ti with enhanced ductility. This value of CP Ti fatigue strength is very high because this level is higher than that for some Ti alloys.

3.2. The Ti-6Al-4V ELI alloy

The alloy processing was conducted on the rods 40 mm in diameter made from the Ti-6Al-4V ELI alloy (Intrinsic Devices Company USA) of the following composition: Ti – base, Al – 6.0%; V – 4.2%; Fe – 0.2%; C – 0.001%; O_2 – 0.11%; N_2 – 0.0025%; H_2 – 0.002%. This alloy with low impurity content is applied for the production of medical implants. The

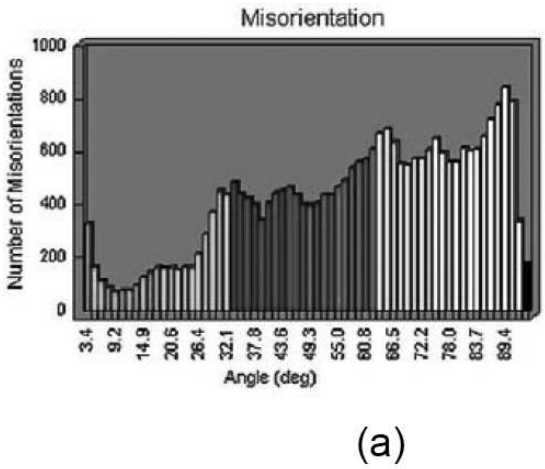

Fig. 2. Distribution of GBs along the misorientation angles in UFG Ti Grade 4 and microstructure after TMT at 450 °C (a and b, respectively).

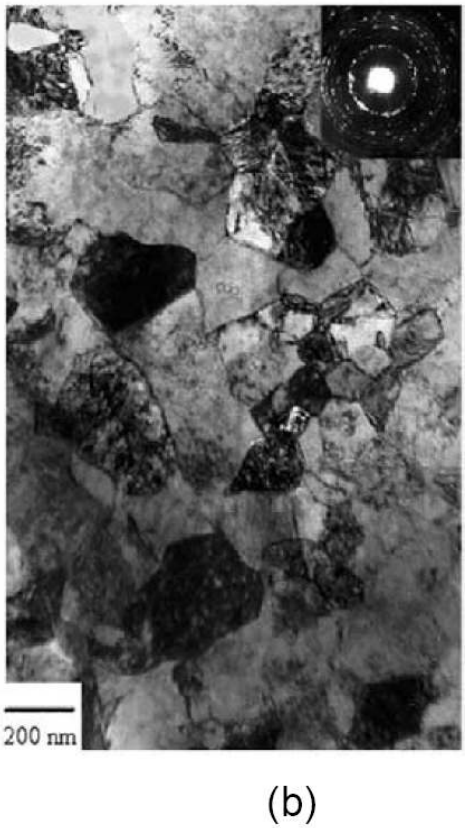

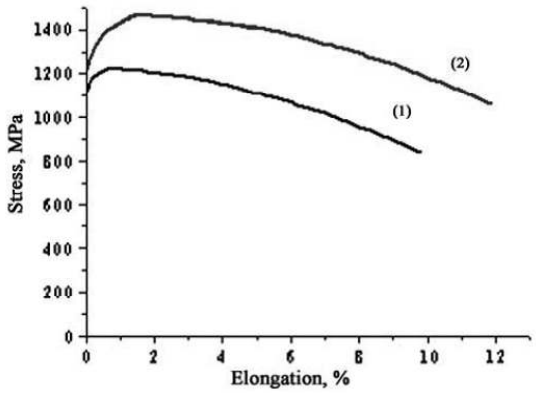

Fig. 3. Typical tensile engineering stress-strain curves for UFG Ti Grade 4 (samples with gage section 2 x 1 x 0.5 mm) after TMT at 200 and 450 °C (1 and 2, respectively).

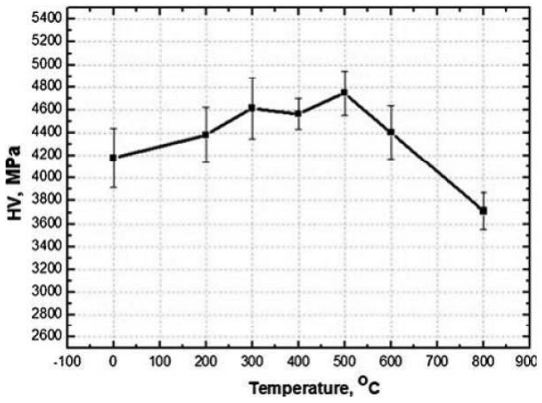

Fig. 4. Dependence of microhardness of the UFG Ti-6Al-4V alloy on the annealing temperature for 1 hour.

temperature of polymorphic transformation (T_{PT}) in the alloy constitutes 960 °C. The microstructure of the alloy in the as-received state had a granular type with an average size of α - grains about 8 μm in cross section, 20 μm in longitudinal section. According to the X-ray diffraction analysis, the volume fraction of α and β phases comprised about 85 and 15% correspondingly. The rods 250 mm in length were subjected to processing in 2 stages: ECAP in a die-set with channels intersection angle φ =120° at a temperature of 600 °C via B_c route and multicycle extrusion at 300 °C with total elongation ratio λ = 4.2 [12].

3.2.1. Microhardness

Fig. 4 illustrates the dependence of microhardness of the alloy subjected to combined SPD-processing on the annealing temperature for 1 hour. Changes in microhardness are seen to be non - monotonic and its increase from 4200 up to 4780 MPa takes place when the annealing temperature is increased up to 500 °C. When the annealing temperature is increased up to 600 °C and higher, microhardness is decreased. Such an unusual strength enhancement in nanostructured materials after annealing was observed earlier in [15,17-19]. The authors of [15] associate the unusual enhancement of strength and ductility of nanostructured Ti after annealing with changes in the structure of grain boundaries. It may be also true for this alloy. Besides, strengthening of the UFG Ti-6Al-4V ELI alloy after annealing at 500 °C can be associated with precipitation of secondary disperse particles or α-phase or alloying elements segregation at grain boundaries as a result of ageing. Therefore, further investigations of microstructure and mechanical properties of the alloy during tensile tests were conducted before and after annealing at 500 °C.

3.2.2. Microstructure and mechanical properties.

Fig. 5 represents the alloy's structure after ECAP and extrusion. SPD processing is seen to lead to considerable grain refinement and formation of a complex UFG structure with grains and subgrains with a mean size of about 300 nm and irregular form, great number of various defects in the crystal lattice and a high level of internal elastic stresses. The elongated grains/subgrains are seen in the longitudinal section determined by extrusion straining (Figs. 5a and 5c). Grain boundaries do not have clear diffraction banded contrast and their images are not well defined indicating the formation of non-equilibrium grain boundaries [2], i.e. the grain boundaries with excess energy and long-range stresses due to the appearance of extrinsic GB dislocations.

Figs. 5d-5f demonstrates that annealing at 500 °C of the alloy subjected to ECAP and extrusion led to significant structure changes, particularly in the longitudinal section of the rod, which are characterized by a clearer boundary contrast and equiaxed grain shape without changes in their mean size. Herewith internal elastic stresses and dislocation density were considerably reduced in the

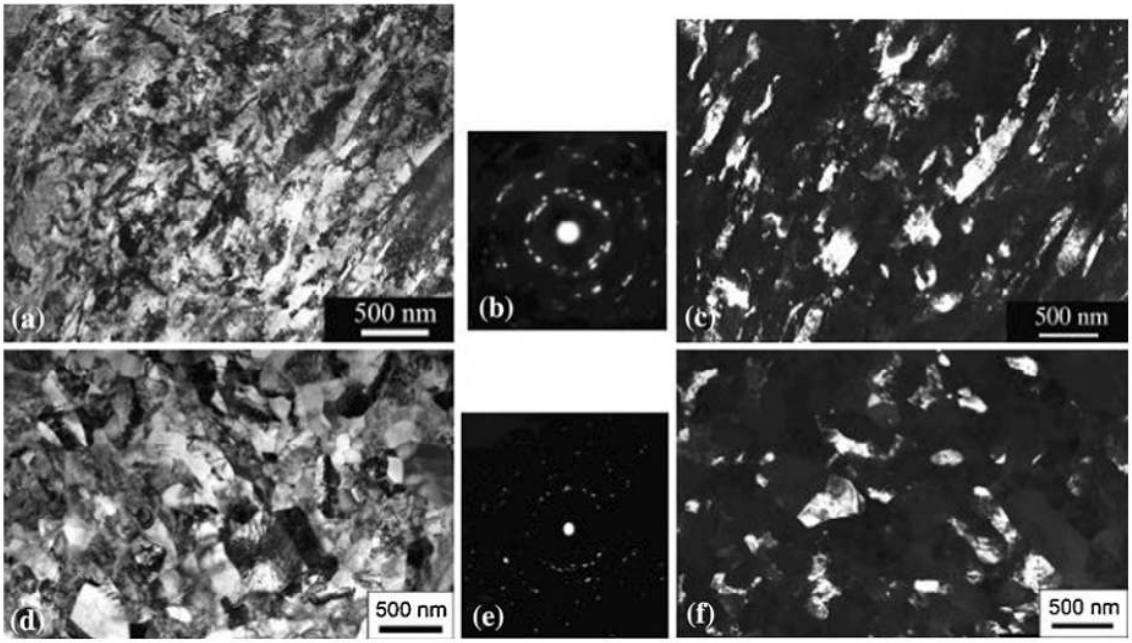

Fig. 5. Microstructure of the UFG Ti-6Al-4V ELI alloy before (a, b, c) and after annealing at 500 °C, 2 hours (d, e, f). Longitudinal section. a, d and c, f – light - field and dark - field images respectively, b, e – SAED patterns. TEM.

structure as evidenced by decrease in azimuthal spot spreading seen in SAED patterns (Figs. 5b and 5e) that was caused by recovery of GB structure to more equilibrium state during annealing.

Fig. 6a displays typical stress - strain curves for the UFG alloy that testify to significant strengthening of the alloy after SPD processing due to microstructure refinement. Tensile elongation becomes less (8%) compared to the initial alloy (15%), but uniform elongation comprised no less than 3%. At the same time subsequent annealing allowed increasing additionally strength and ductility (up to

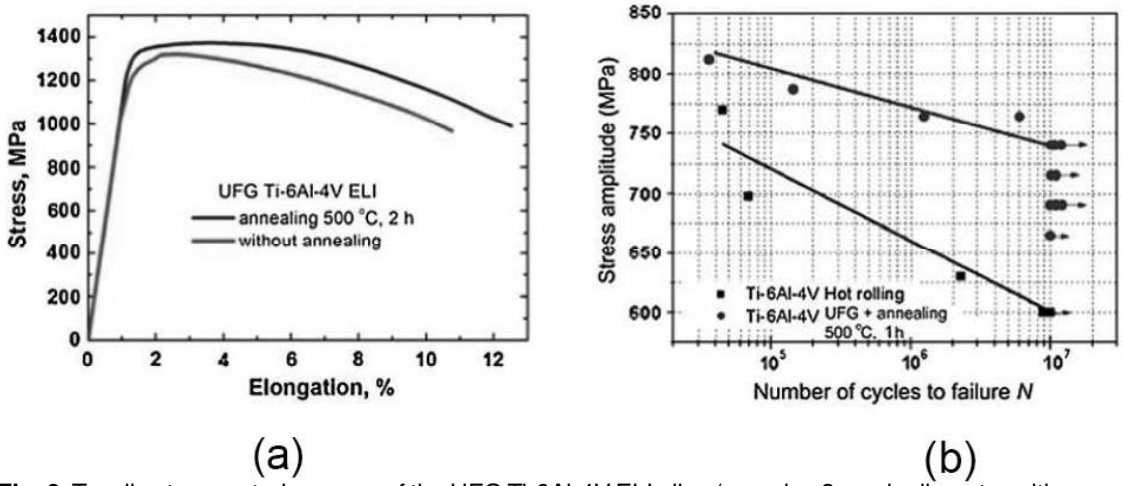

Fig. 6. Tensile stress - strain curves of the UFG Ti-6Al-4V ELI alloy (samples 3 mm in diameter with a gage section of 15 mm) before and after annealing at 500 °C (a) and fatigue test results of the smooth samples out of CG and UFG alloy (samples 65 mm in total length, diameter of gage section 3 mm) after annealing at 500 °C, 2 hours (b).

12%), namely uniform elongation up to 4%. Therefore the formation of equiaxed ultrafine grains and more equilibrium grain boundaries, clearly seen in TEM picture, contributes to strength and ductility enhancement. This phenomenon has already been discussed in detail elsewhere [5,6]. In UFG materials with low strain-rate sensitivity during the deformation, developing of more equilibrium grain boundaries contributes to strain hardening due to enhancement of dislocations accumulation. Though there are no visible particles of any second phase, aging processes could lead to the formation of grain boundary segregations or precipitations that could also additionally contribute to enhancement of properties of the UFG alloy subjected to annealing. Recently such experiments have been implemented during aging of the UFG Al alloys [20,21].

Investigations of fatigue properties of the UFG Ti-6Al-4V ELI alloy revealed that high strength and enhanced ductility after SPD processing and additional annealing at 500 °C resulted in fatigue limit enhancement on the basis of 10^7 cycles up to 740 MPa in comparison with 600 MPa in the initial coarse - grained (CG) state (Fig. 6b).

3.3. The Al 1570 alloy

An important feature of the UFG Al alloys produced by SPD techniques is also the occurrence of non-equilibrium GBs [2]. It is of particular importance because it contributes to the formation of GB segregations and precipitations and as a result produces a considerable effect on the mechanical properties of UFG materials. The convincing argument for that is the study of the UFG Al alloy 1570 [13] subjected to HPT under different temperatures – the room temperature, 100 °C and 200 °C.

It is established that after HPT at room temperature and HPT at 100 °C, practically identical structures were formed with the average grain size of 130 ± 10 nm (Figs. 7a and 7b). Structure with a higher grain size (210 ± 7 nm) was obtained in billets after processing at 200 °C (Figs. 7c and 7d).

Typical SAED patterns (Figs. 7a and 7c) are multiple spots uniformly distributed along circles. They testify to the fact that the formed states refer to the structures of the granular type with mostly high-angle grain boundaries. A specific diffraction contrast is observed at grain boundaries formed during HPT at room temperature and 100 °C. The diffraction contrast is indicative of non-equilibrium state of grain boundaries [2,22]. At the same time, there are no such structural features in the alloy after HPT at 200 °C (Figs. 7c and 7d), which is evidence for more equilibrium grain boundaries.

HPT processing strongly influences the value of the lattice parameter (*a*) of the alloy crystal lattice. Its value decreases significantly after straining and approaches to the parameter of pure Al. The most considerable decrease of *a* (by ~ 0.2%) as compared to the initial state occurs after HPT treatment conducted at elevated temperatures.

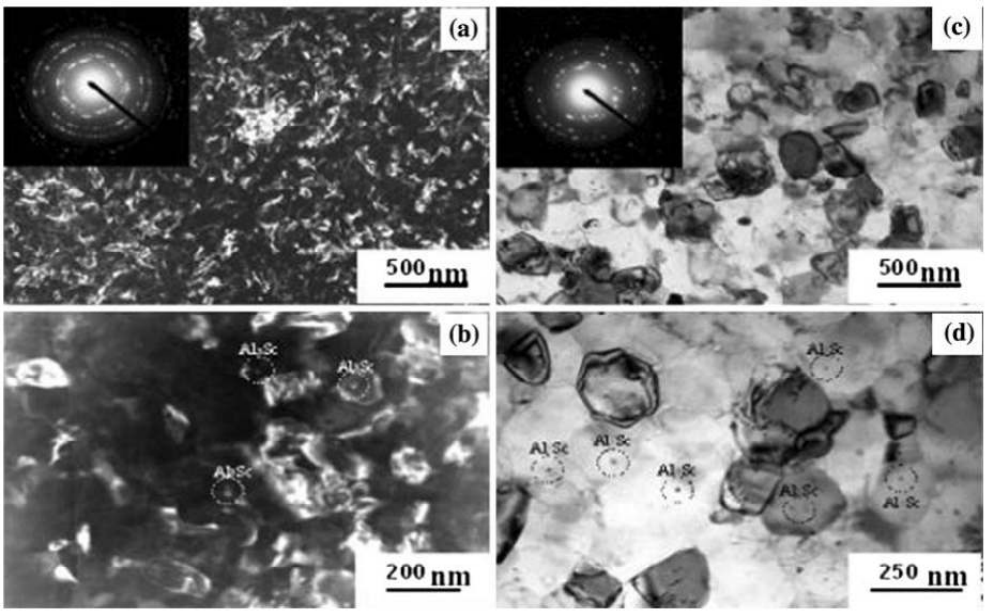

Fig. 7. Microstructure of the 1570 alloy processed by HPT at room temperature (a, b) and at 200 °C (c, d).

The reduction of the crystal lattice parameter of Al-Mg alloys is associated with decrease of Mg content in the solid solution [23]. Herein, decreasing of Mg concentration by 1 at.% results in the change of *a* by 0.0046 Å [24]. Thus, taking into account by the established changes in *a*, 1570 solid solution after HPT processing at room temperature lost about 1.6 at.% of Mg. It is natural to suppose that due to dislocation activity Mg atoms were dragged to grain boundaries to form segregations [25]. This suggestion had been recently confirmed by direct atomic-scale observations with the help of 3D atom probe analysis [21].

As it was observed from the mechanical tests, the UFG 1570 alloy after HPT at room temperature demonstrates superior strength that is more than twice as higher as the strength of the material subjected to standard hardening (Fig. 8). The exhibited strength values exceeds those of conventional high-strength heat-treated Al alloys of a Al–Zn–Mg–Cu system [26] and a number of UFG Al alloys produced earlier [27,28]. The strength of the UFG 1570 alloy is even higher than it follows from the Hall-Petch dependence (Fig. 9), which indicates the presence of additional factors leading to alloy hardening.

As TEM observations provide no evidence of the formation of any disperse phases after HPT such unusual change in the mechanical properties of the UFG alloy is likely associated with the segregations of solute elements along the boundaries of formed UFG grains.

This phenomenon can be explained by the assumption that emission of dislocations from grain boundaries is impeded by formation of segregations.

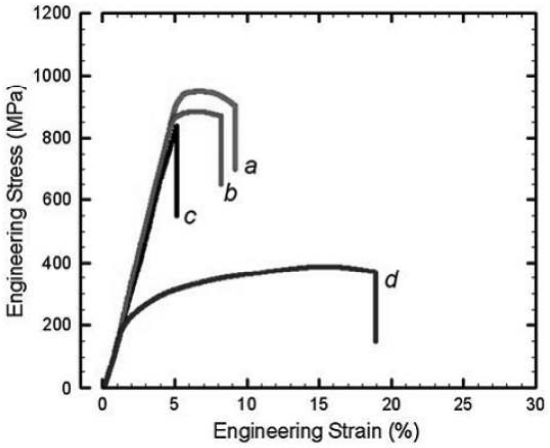

Fig. 8. Tensile curves of the Al 1570 alloy (samples with gage section 2 x 1 x 0.5 mm) processed by HPT at room temperature (a), 100 °C (b), 200° (c) and initial state (d).

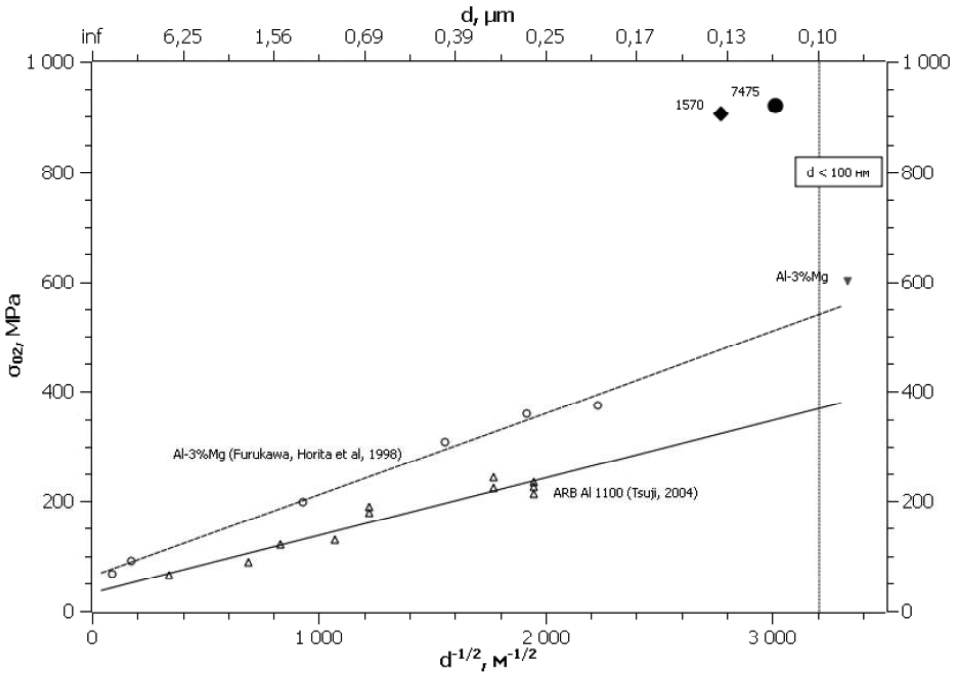

Fig. 9. The Hall-Petch relation for the alloys 1100 [52], Al-3%Mg [53] and data on the yield stresses of the UFG alloys 1570 and 7475.

The critical stress for the emission of an individual dislocation may be expressed as [29]:

$$\sigma = \alpha \frac{Gb}{L}\left[\ln\frac{L}{b} - 1.65\right], \quad (1)$$

where σ is the flow stress, G is the shear modulus, b is the Burgers vector, L is dislocation line or source length, α is a constant.

For the deformation by dislocation movement, L can be expressed by $L=\upsilon/b^2$, where υ is the activation volume, which in its turn is related to strain rate sensitivity m [29]:

$$m = \frac{\sqrt{3}kT}{\sigma\upsilon}, \quad (2)$$

where k is the Boltzmann constant and T – temperature.

For the experimentally measured strength of the UFG 1570 alloy, the maximum flow stress, necessary to emit a dislocation from a grain boundary is achieved (1) at $\upsilon \sim 15b^3$, which according to (2) corresponds to m~0.02. This strain rate sensitivity value is similar to experimentally measured one for the case of UFG Al alloys at ambient temperature [30] which confirms the suggested mechanisms of the alloy enhanced strength.

The mechanical tests of the UFG 1570 alloy at elevated temperatures were performed to study its superplastic behavior. The tensile tests were carried out on an automated testing machine (P6735) at various temperatures (300, 350, and 400 °C) and a constant velocity of the moving clamp [31]. After HPT, all tensile tested samples of the UFG alloy exhibited superplasticity at strain rates that were several orders higher as compared to those for the initial CG samples. At 300 °C, the maximum elongation to failure (δ = 580%) is achieved at $\dot{\varepsilon} = 10^{-1}$ s^{-1}, and at 350 °C, the maximum δ = 800% is achieved at $\dot{\varepsilon} = 1.8\times10^{-1}$ s^{-1}. The deformation behavior of the UFG alloy at 300 and 350 °C obeys the well-known correlation between $m(\dot{\varepsilon})$ and $\delta(\dot{\varepsilon})$ curves. The maximum values of the strain-rate sensitivity coefficient at these temperatures (m~0.38 and 0.42 respectively) are achieved at the strain rates close to those corresponding to the maximum ductility.

4. DISCUSSION

The obtained results demonstrate clearly a strong influence of GB structure on the mechanical behavior and properties of UFG metals and alloys produced by SPD techniques. As it has already been mentioned in the introduction, primarily, the concept of GB engineering or GB design was introduced by Watanabe in [8], where it has been proposed that the properties of polycrystalline materials may be effectively changed by deliberate and careful tailoring of the grain boundary character distribution. The goal of the primarily proposed grain boundary engineering was to increase volume fraction of so-called special boundaries at the expense of random large angle boundaries in the processed material. Special boundaries are recognized by low reciprocal number density of lattice sites, (Σ) and corresponding misorientaion angle as described by coincidence site lattice (CSL) model [32]. These boundaries possess significantly reduced energy as compared to the random ones and grain boundary engineering can influence the manifested properties of the material [8,33,34]. For example, substantial enhancements in corrosion resistance [35,36], creep resistance [37-41] and stress corrosion cracking resistance [34,42-44] have been correlated with the increase in special boundary fraction in grain boundary engineered materials. One of the most common methodical approaches to grain boundary engineering is the formation of annealing twins (bounded by coherent Σ3 boundaries) which contributes directly to the increase in special boundaries fraction, as well as indirectly, when twin boundaries interact with random boundaries to produce low-Σ boundaries [45,46].

Hereafter several attempts have been taken on extension of grain boundary engineering concept by other possibilities of influencing the GB structure. In [47] the authors suggested to consider the aspects of grain boundary formation beyond the scope of the original GB engineering concept, which exploits “low-Σ - low grain energy” relation. In particular, it was suggested to consider the effects connected with GB free volume change, triple junctions mobility and segregations formation. Such a modified approach extends the initial GB engineering idea and provides advanced possibilities of influence on materials properties through the modification of their GB structure.

Development of GB engineering approaches can be especially prominent being applied to UFG and nanostructured materials, where the significantly increased grain boundary fraction can drastically affect the materials properties. For example, variation of GB distribution by type accompanied with introduction of GB segregations essentially influenced the embrittlement behaviour of the UFG Ni [48].

The results of the presented work testify that, SPD techniques can provide a cardinally new possibilities for GB engineering as grain boundary structure features in the SPD materials are strongly dependant on processing regimes. For example, there is a possibility to control a grain boundary misorientation distribution producing materials consisted preferably of low-angle or high-angle boundaries that considerably affects their diffusion properties [49]. Besides, it is revealed that enhanced superplasticity at relatively low temperatures or/and high strain rates is only observed in UFG materials with high-angle grain boundaries and is not observed when low-angle grain boundaries fraction exceeds 50% [50].

Moreover, SPD reveals absolutely new perspectives for grain boundary engineering because as it was stated above, it is capable to affect grain boundary structure by formation of non-equilibrium states in boundaries and precipitations/segregations in interface regions [2,6]. Recent studies [51] as well as the results of the given work show that SPD techniques have a high potential to work out and successfully fulfill new principles for GB engineering of UFG materials.

5. CONCLUSIONS

Thus, a strong influence of GB structure on the mechanical behavior and properties of UFG metals and alloys produced by SPD techniques is demonstrated. The parameters of GB structure include the fraction of low- and high-angle boundaries, presence of non-equilibrium grain boundaries associated with the extrinsic GB dislocations and also the formation of segregations along the boundaries. The GB structure in its turn is closely related to the SPD processing routes and regimes. The examples reported testify that GB engineering of UFG materials by SPD processing can be a very promising approach to enhance their properties and requires further detailed studies.

REFERENCES

[1] H. Gleiter // *Prog. Mater. Sci.* **33** (1989) 223.
[2] R. Z. Valiev, R. K. Islamgaliev and I. V. Alexandrov // *Prog. Mater. Sci.* **45** (2000) 103.
[3] Y.H. Zhao, J.F. Bingert, Y.T. Zhu, X.Z. Liao, R.Z. Valiev, Z. Horita, T.G. Langdon, Y.Z. Zhou and E.J. Lavernia // *Appl. Phys. Lett.* **92** (2008) 081903.
[4] S.V. Divinski, J. Ribbe, D. Baither, G. Schmitz, G. Reglitz, H. Rosner, K. Sato, Y. Estrin and G. Wilde // *Acta Mater.* **57 (**2009) 5706.
[5] R. Valiev // *Nature Mater.* **3** (2004) 511.
[6] R. Valiev // *Mater. Sci. Forum* **584-586** (2008) 22.
[7] I.A. Ovid'ko and A.G. Sheinerman // *Acta Materialia* **57(7) (**2009) 2217.
[8] T. Watanabe // *Res. Mech.* **11** (1984) 47.
[9] T. Watanabe, H. Fujii, H. Oikawa and K.I. Arai // *Acta Metall.* **37** (1989) 941.
[10] R.Z. Valiev and T.G. Langdon // *Prog. Mater. Sci.* **51** (2006) 881.
[11] R.Z. Valiev, I.P. Semenova, E.B. Yakushina, V.V. Latysh, H. Rack, T.C. Lowe, J. Petruzelka, L. Dluhos and J. Sochova // *Mater. Sci. Forum* **584-586** (2008) 49.
[12] I.P. Semenova, L.R. Saitova, G.I. Raab, A.I. Korshunov, Y.T. Zhu, T.C. Lowe and R.Z. Valiev // *Mater. Sci. Forum* **503-504** (2006) 757.
[13] M.Yu. Murashkin, A.R. Kilmametov and R.Z. Valiev // *Phys. Metal. Metallogr.* **106(1) (**2008) 93.
[14] O.B. Kulyasova, R.K. Islamgaliev and R.Z. Valiev // *Phys. Met. Metallogr.* **100** (2006) 277.
[15] R. Valiev, A.V. Sergueeva and A.K. Mukherjee // *Scripta Mater.* **49** (2003) 669.
[16] R.Z. Valiev, I.V. Alexandrov, Y.T. Zhu and T.C. Lowe // *JMR* **17** (2002) 5.
[17] R.Z. Valiev, F. Chmelik, F. Bordeaux, G. Kapelski and B. Baudelet // *Scripta Metall. Mater.* **27** (1992) 855.
[18] J. Languillaume, F. Chmelik, G. Kapelski, F. Bordeaux, A.A. Nazarov, G. Canova, C. Esling, R.Z. Valiev and B. Baudelet // *Acta Metall. Mater.* **41** (1993) 2953.
[19] A.A. Popov, I. Yu. Pyshmintsev, S.L. Demakov, A.G. Illarionov, T.C. Lowe, A.V. Sergeyeva and R.Z. Valiev // *Scripta Mater.* **37** (1997) 1089.
[20] R.Z. Valiev, M.Yu. Murashkin, E.V. Bobruk and G.I. Raab // *Mater. Trans.* **50** (2009) 87.
[21] G. Nurislamova, X. Sauvage, M. Murashkin, R. Islamgaliev and R. Valiev // *Phil. Mag. Lett.* **88** (2008) 459.
[22] R.Z. Valiev and I.V. Alexandrov, *Bulk nanostructured metallic materials* (Akademkniga publ., Moscow, 2007), p.398.
[23] L.N. Gusev, M.F. Nikitina, L.K. Dolinskaya and I.V. Egiz // *Izvestiya AS USSR, Metaly*, (Russian metals) **4** (1972) 208.

[24] *Aluminium: properties and physical metallurgy,* ed. by J.E. Hatch (American Society for Metals, Metals Park, Oh., 1984), p. 422.
[25] L.V. Gapontsev, I.K. Razumov and Yu.N. Gornostyrev // *FMM* **99(4) (**2005) 26.
[26] Z.N. Archakova, G.A. Balakhontsev and I.G. Basova, *Structure and properties of Aluminium alloy semifinished product. Handbook, 2nd ed.* (Metallurgia, Moscow, 1984), p.408.
[27] M.V. Markushev and M.Yu. Murashkin // *Phys. Met. Metallogr.* **5** (2000) 506.
[28] H. J. Roven, H. Nesboe, J.C. Werenskiold and T. Seibert // *Mater. Sci. Eng.* **A410–411 (**2005) 426.
[29] J. Lian, C. Gu, Q. Jiang and Z. Jiang // *Journal of Applied Physics* **99** (2006) 0761031.
[30] R. Hayes, D. Witkin, F. Zhou and E. Lavernia // *Acta Mater.* **52** (2004) 4259.
[31] V.N. Perevezentsev, M.Yi. Shcherban, M.Yu. Murashkin and R.Z. Valiev // *Tech. Phys. Lett.* **33** (2007) 648.
[32] H. Grimmer, W. Bollman and D.H. Warrington // *Acta Crystallographica* **A30 (**1974) 197.
[33] G. Palumbo, E.M. Lehockey and P. Lin // *JOM* **50** (1998) 40.
[34] A.J. Schwartz and W.E. King // *JOM* **50** (1998) 50.
[35] G. Palumbo and K.T. Aust // *Acta Metall. Mater.* **38** (1990) 2343.
[36] P. Lin, G. Palumbo, U. Erb and K.T. Aust // *Scripta Metall. Mater.* **33 (**1995) 1387.
[37] T. Watanabe // *Metall. Trans. A.* **14** (1983) 531.
[38] H. Kokawa, T. Watanabe and S. Karashima // *Phil. Mag. A.* **44** (1981) 1239.
[39] E.M. Lehockey, G. *Palumbo* // *Mater. Sci. Eng. A* **237** (1997) 168.
[40] G.S. Was , V. Thaveeprungsriporn and D.C. Crawford // *JOM* **50** (1998) 44.
[41] E.M. Lehockey, G. Palumbo, A. Brennenstuhl and P. Lin // *MRS Symp. Proc.* **458** (1997) 243.
[42] D.C. Crawford and G.S. Was // *Metall. Trans. A.* **23** (1992) 1195.
[43] B. Alexandreanu, B. Capell and G.S. Was // *Mater. Sci. Eng. A.* **300** (2001) 94.
[44] G. Palumbo, P.J. King, K.T. Aust, U. Erb and P.C. Lichtenberger// *Scripta Metall. Mater.* **25** (1991) 1775.
[45] V.Y. Gertsman and K. Tangri // *Acta Metall. Mater.* **43** (1995) 2317.
[46] P. Lin, G. Palumbo and K.T. Aust // *Scripta Mater.* **36** (1997) 1145.
[47] L.S. Shvindlerman and G. Gottstein // *Scripta Mater.* **54** (2006) 1041.
[48] S. Kobayashi, S. Tsurekawa, T. Watanabe and G. Palumbo // *Scripta Mater.* **62** (2010) 294.
[49] T. Fujita, Z. Horita and T.G. Langdon // *Mater Sci Eng. A* **371** (2004) 241.
[50] R.K. Islamgaliev, R.Z. Valiev, R.S. Mishra and A.K. Mukherjee // *Mater Sci Eng .A.* **304-306** (2001) 206.
[51] R.Z. Valiev, M.Yu. Murashkin and I.P. Semenova // *Metall. Mater. Trans.* **41 A 4** (2010) 816.
[52] N. Tsuji, In: *Nanostructured Materials by High-Pressure Severe Plastic Deformation*, ed. by Y. T. Zhu and V. Varyukhin (Springer Netherlands. 2006), p. 227.
[53] M. Furukawa, Z. Horita, M. Nemoto, R.Z. Valiev and T.G. Langdon // *Phil. Mag. A.* **78** (1998) 203.